The use of liquid crystal thermography TLC and particle image velocimetry PIV in selected technical applications

JAN A. STĄSIEK[*]
MARCIN JEWARTOWSKI

Gdańsk University of Technology, 80-233 Gdańsk, Narutowicza 11/12, Poland

Abstract Nowadays, the energy cost is very high and this problem is carried out to seek techniques for improvement of the aerothermal and thermal (heat flow) systems performances in different technical applications. The transient and steady-state techniques with liquid crystals for the surface temperature and heat transfer coefficient or Nusselt number distribution measurements have been developed. The flow pattern produced by transverse vortex generators (ribs) and other fluid obstacles (e.g. turbine blades) was visualized using liquid crystals (Liquid Crystal Thermography) in combination with the true-colour image processing as well as planar beam of double-impulse laser tailored by a cylindrical lens and oil particles (particle image velocimetry or laser anemometry). Experiments using both research tools were performed at Gdańsk University of Technology, Faculty of Mechanical Engineering. Present work provides selected results obtained during this research.

Keywords: Liquid crystal thermography; Particle image velocimetry; Heat transfer; Fluid flow visualization

1 Introduction

The beginning of the 21st century is a period of intense scientific and research work related to micro- and nanotechnology, a highly effective technology of energy conversion and methods of limiting its impact on the

---

[*]Corresponding Author. Email:jstasiek@pg.gda.pl

degradation of the natural environment. Scientific teams dealing with heat and mass exchange must face new challenges in the design and construction of modern and highly effective process equipment. Typical and idealized cases reported in the professional literature are no longer sufficient to solve current technical or technological problems. Citing, for example, two of them: cooling gas turbine blades or cooling electronic systems, are associated with complex geometry, heterogeneous boundary conditions, and the action of aggressive and usually non-stationary flow. Designers of thermal equipment now expect more accurate information not only about average heat transfer coefficient but also about its local values. These expectations are met by automated and fully computerized optical measurement methods, like infrared thermography [1] or liquid crystal thermography [2]. Both of them are widely used in temperature measurements during single and two-phase flow heat transfer investigations, especially in mini- and microscale. They allow precise observation of complex phenomena and are essential for their mathematical description or validation of proper models [3,4]. Liquid crystal thermography based on physicochemical properties of liquid crystal as well as digital and analogue analysis of colour images allow not only to study complex geometries or the influence of inhomogeneous boundary conditions, but also pulsatile and turbulent flows of large scales and low frequencies. Situations with such a complex heat exchange can be found in most devices in which energy conversion processes occur. Analog-digital liquid crystal thermography and particle image velocimetry are excellent and recognized measurement methods used in major scientific centers in the world and in Poland. They enable visualization of two-dimensional temperature and velocity fields with an accuracy of one pixel and learning the influence of many thermophysical and flow factors on the formation of laminar and turbulent boundary layer.

2 Liquid crystals thermography

Liquid crystals constitute a class of matter unique in exhibiting mechanical properties of liquids (fluidity and surface tension) and optical properties of solids (anisotropy to light, birefringence). Although they were first observed more than 120 years ago by an Austrian botanist, Friedrich Reinitzer, studies of liquid crystals were confined to material laboratories until the 60's when applications to science and engineering began [5].

The original use of the term 'liquid crystal' is credited to Lehman, a Ger-

man physicist. In many publications of the time, Lehman used terms like *Fliesende Krystalle* (flowing crystals) and *Flussige Krystalle* (fluid crystals) to describe the unusual phase that existed between the two melting points of not only cholesteryl benzoate, but also a large number of other compounds he studied.

Liquid crystals are temperature indicators that modify incident white light and display colour whose wavelength is proportional to temperature. They can be painted on a surface or suspended in the fluid and used to make visible the distribution of temperature. Normally clear, or slightly milky in appearance, liquid crystals change in appearance over a narrow range of temperature called the 'colour-play interval' (the temperature interval between first red and last blue reflection), centered around the nominal 'event temperature'. The displayed colour is red at the low temperature margin in the colour-play interval and blue at the high end. Within the colour-play interval, the colours change smoothly from red to blue as a function of temperature [6]. The effect is reversible which, in practical terms, means that a single application of liquid crystals to a model can be used repeatedly (usually until coating is oblated or otherwise damaged). Both the colour play interval and the event temperature range of a liquid crystal can be selected by adjusting its composition, and materials are available with event temperatures from -30 °C to 120 °C and with colour play bands from 0.5 °C to 20 °C [6,7] although not all combinations exist of event temperature and colour play band widths. Widths of 1 °C or less will be called narrow band materials, while those whose band width exceeds 5 °C will be called wide band. The types of material to be specified for a given task depend on the type of used image interpretation technique [8].

Liquid crystals are classified into three categories according to their molecular structures: smectic, nematic, and cholesteric. However, from a structural viewpoint, it can be argued that there are only two basic types of liquid crystals, chiral-nematic and smectic, with cholesteric being regarded as a special kind of nematic. Their structures are shown schematically in Fig. 1 [7]. For flow analysis the suspension of thermochromic liquid crystals (TLC) can be used to make visible the temperature and velocity fields in liquids. By dispersing the liquid crystal material into the liquid they become not only classical tracers used for flow visualisation but simultaneously small thermometers monitoring local fluid temperature [9]. A collimated source of white light must be used to illuminate a selected cross-section of the flow (light sheet technique) and colour images
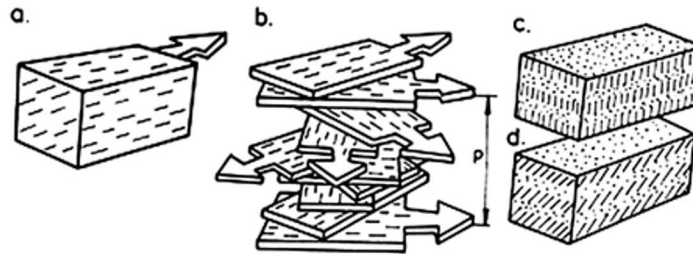
Figure 1: A different view of the mesophase structure. The orientation of the molecular
director is represented by the arrows: a – nematic, b – cholesteric, c – smectic
A, d – smectic B [7].

are acquired in a perpendicular direction. In the following examples the
un-encapsulated TLC's tracers have been applied to measure both tem-
perature and velocity flow fields. It was found that light scattered by the
capsule shell inevitably diminishes saturation of the observed colours. Be-
cause in a slow motion the stress effects are negligible we prefer application
of fine dispersed raw material in flow measurements.

To get the qualitative information about temperature field an image
analysis is necessary. Some publications described the suitability of colour
space transformations for such optical temperature measurements [10]. Ma-
ny image processing operations developed for processing grey-level (inten-
sity) images can be readily applied to HSI (hue saturation intensity)colour
images. These include image transformations, enhancements, analysis,
compression and restoration. A schematic view of image processing sys-
tem (developed by one of the authors) can be found in [11].

Before the execution of a thermal or flow visualization experiment, we
should recognize the characteristics of the overall combination of TLC, the
light source, the optical camera system (ordinary, CCD (charge-coupled
device) black and white or RGB camera), and make a rational plan for the
total measurement system. The relationship between the temperature of
the crystal and the measured hue of the reflected lights defines the calibra-
tion curve for the liquid crystal. The result is a curve relating the hue of
the reflected light to the surface temperature. A known temperature dis-
tribution exists on a 'calibration plate' (brass plate) to which is attached
the light crystal layer. In order to maintain a linear temperature distri-
bution with desired temperature gradients, one end of a brass plate was

cooled by stabilized water and the other end controlled electrically [12,13]. The brass plate with the liquid crystal layer is calibrated in place in the wind tunnel with the same lighting level and viewing angle used during the data acquisition phase of the experiment [13]. The distribution of the colour component pattern on the liquid crystal layer was measured by RGB colour camera and series of images at a different temperatures defines the calibration [11]. More information about calibration of liquid crystal can be also found in [14].

In recent years liquid crystals were used among others in research of flow and heat transfer in ribbed channels [15,16], turbine cascade blades [17] or as temperature sensors in the case of investigations in strong magnetic field [18]. Magnetic field was the source of additional force, which was able to enhance heat transfer of paramagnetic fluids connected directly with temperature changes indicated by the liquid crystals.

Two main methods of surface temperature measurement are used in Gdańsk University of technology, that is steady-state and transient techniques.

2.1   Steady-state analyses – constant flux method

The steady-state techniques employ a heated model and the TLC is used to monitor the surface temperature. Usually a surface electric heater is employed such that the local flux, q, is known and this, together with the local surface temperature, T_w, (found from the TLC), gives the local heat transfer coefficient, h:

$$q = I^2 r \tag{1}$$

and

$$h = \frac{q}{T_a - T_w} \ , \tag{2}$$

where T_a is a convenient driving gas temperature, I is the current and r is the electrical resistance per square of the heater.

2.2   Steady-state analyses – uniform temperature method

The TLC-coated test specimen forms one side of a constant temperature water bath and is exposed to a cool/hot air flow. The resulting thermograph is recorded on film or video and further measurement positions are obtained by adjusting the water bath temperature. This method is more time consuming due to the large volume of water that needs to be heated.

In this case, the heat transfer coefficient is determined by equating convection to the conduction at the surface

$$h\left(T_a - T_w\right) = \frac{k}{x}(T_w - T_b) \, , \tag{3}$$

where T_b is a water-side temperature of the wall, x, the wall thickness, and k the thermal conductivity.

2.3   Transient method

This technique requires measurement of the elapsed time to increase the surface temperature of the TLC-coated test specimen from a known initial value of predetermined temperature. The rate of heating is recorded by monitoring the colour change patterns of the TLC with respect to time. If the specimen is made from a material of low thermal diffusivity and chosen to be sufficiently thick, then the heat transfer process can be considered to be one-dimensional (1D) in a semi-infinite block. Numerical and analytical techniques can be used to solve the 1D transient conduction equation. The relationship between wall surface temperature, T, and heat transfer coefficient, h, for the semi-infinite case is

$$\frac{T - T_i}{T_a - T_i} = 1 - e^{\beta^2}\text{erfc}(\beta) \tag{4}$$

$$\beta = h\left(\frac{t}{\rho c k}\right)^{0.5} \tag{5}$$

where ρ, c, and k are the model density, specific heat and thermal conductivity. T_i and T_a are the initial wall and gas temperatures, respectively, and t is time from initiation of the flow. More recent formula for evaluation of heat transfer coefficient is given in the following form:

$$h = -\frac{\delta \rho c}{2t} \ln\left[\frac{T_a - T}{T_a - T_i}\right] \, , \tag{6}$$

where δ is a plate wall thickness and the transient local surface temperature T is detected after a time interval t [7,8,11,19].

2.4   Applications

In the following examples the TLC's plastic sheet and capsulated TLC's tracers have been applied to measure both temperature and velocity flow fields. These are only a more couple examples of research performed previously by authors using liquid crystal thermography.

2.4.1   Full field surface temperature measurements

Liquid crystals can be used to determine the distribution of the surface temperature, and if the surface heat flux can be found, this allows evaluation of the heat transfer coefficient or the Nusselt number. The alternative effects of constant wall temperature and constant heat flux boundary conditions are obtained using a water bath. Photographs are taken using a RGB video-camera and a true-colour image processing technique. Usually several isotherms (each corresponding to a different heat flux) are taken by RGB video-camera to record the local Nusselt contours under an oblique Reynolds number. The locations of each isotherm and colour (adjusted to each Nusselt number) are digitised following a projection of the false colour image on a digitising image respectively (this particular method can be called 'image combination technique' ICT). Figure 2 shows photographs of the colour distribution of the liquid crystal layer around a square section column, image of the computer display after segmentation processing (hue: 45–55) and false colour image processing (ICT) respectively on the right.
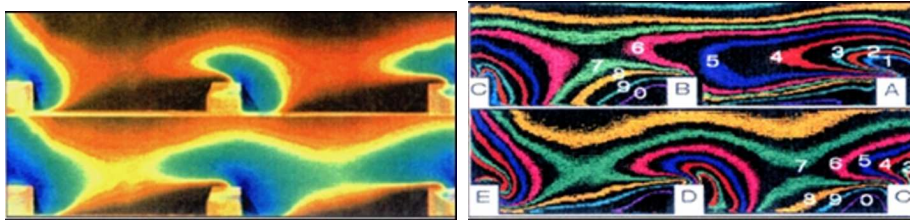

Figure 2: True-colour images from liquid crystal thermography for the endwall surface with in-line square ribs (up). Pattern of 10 Nusselt numbers reconstructed by false colour images of heat.

2.4.2   Natural convection in a closed cavity

Vertical temperature gradients are mainly responsible for the atmospheric or oceanographic fluid motion. Development of the nocturnal stable stratification over flat areas, inversion of temperature gradient and break-up of the convective boundary layer developed at the ground levels can be simulated using small-scale laboratory experiments. One of the typical features characterizing instabilities generated by vertical temperature gradient are plumes or ejections appearing, when the thermal boundary layer breaks up. Figure 3 shows temperature and velocity visualization in glycerol-filled cavity under free convection in horizontal and vertical position.
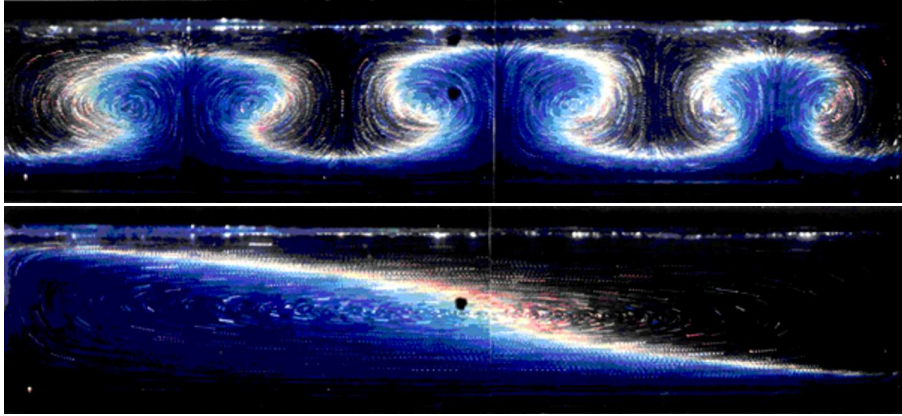
Figure 3: Visualization of Benard cells in the horizontal (top) and vertical (bottom) cavity using TLC.

3 Particle image velocimetry

Particle image velocimetry (PIV) technique is also well-established experimental method in fluid mechanics, that allows quantitative measurement of two-dimensional flow structure.
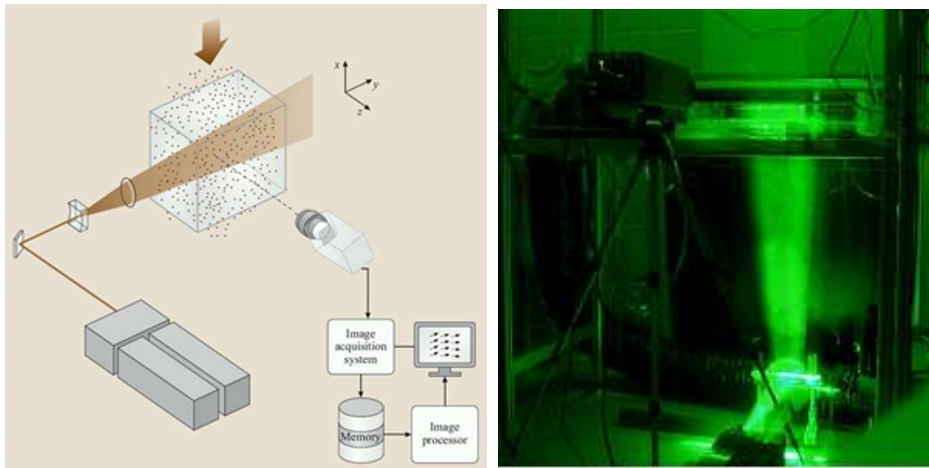

Figure 4: Schematic of a typical PIV measurements (left) and 'laser light sheet' (right).

This technique enables measurements of the instantaneous in-plane velocity vector field within a planar section of the flow field and allows to calculate

spatial gradients, dissipation of turbulent energy, spatial correlations, and the like. In PIV technique selected cross-section of the investigated seeded flow is illuminated by the laser light formed in thin 'light sheet' (Fig. 4). Images of the flow are recorded by CCD camera and correlated to calculate instantaneous velocity fields.

Some of many research performed in recent years using this technique include investigations of impinging jet flows [20], ribbed channels [21,22], micro heat sinks [23] or turbulence in micro-channel emulsifier [24].

4   Experimental facility

Experimental facility has been designed in the form of an open air tunnel and constructed at the Department of Energy and Industry Apparatus of Gdansk University of Technology. Thanks to its universal construction, it allows testing a wide range of geometries with a small amount of resources needed to adapt the measurement section to subsequent experiments. In this case, it was used to study model elements of heat exchangers and in particular passive intensification of heat exchange on finned surfaces. After modification of the measurement section, they were used to investigate the process of cooling of gas turbine blades. Open low-speed wind tunnel consists of entrance section with fan and heaters, large settling chambers with diffusing screen and honeycomb, and then working sections (Fig. 5). Air is drawn through the tunnel using a fan able to attain the Reynolds numbers in the range from 500 to 40 000. The working air temperature in the rig ranges from 15 °C to 65 °C is produced by the heater or cooler positioned just downstream of the inlet. The major construction material of the wind tunnel is perspex. Local and mean velocity are measured using conventional Pitot tubes and DISA hot-wire velocity probe.

The alternative effects of constant wall temperature and constant heat flux boundary conditions are obtained using the plate electric heater. Photographs are taken using RGB video-camera and a true-colour image processing technique. The liquid crystals used here, manufactured in sheet form by Hallcrest [25], had an event temperature range from 30 to 35 °C. In this particular experiment uncertainty for temperature measurement was estimated at about ±0.05 °C by considering only the section of the surface used in the experiment, span-wise non-uniformities in hue value are minimized.
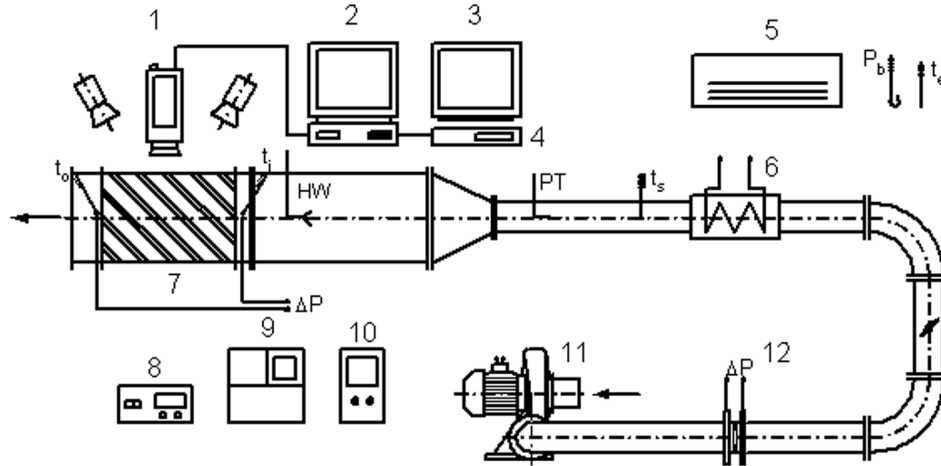
Figure 5: Open low speed wind tunnel, 1 – RGB camera (TK-1070), 2 – PC computer, 3
– monitor (RGB-VMR 200), 4 – S-VHS recorder, 5 – air conditioning system,
6 – heater, 7 – liquid crystals mapping section, 8 – digital micromanometer
FCO 12, 9 – DISA hot wire system, 10 – variac, 11 – fan, 12 – orifice.

In many cases, remarkable enhancement of local and spatially averaged
surface heat transfer rates are possible with rib turbulators, in spite of
the lower local Nusselt number at certain locations along the ribbed sur-
faces. For that measurements test section is prepared, as a flat channel
with a width of 254 mm and a height of 40 mm and length 550 mm made
of plexiglass with a thickness of 8 mm. The test surface that is analyzed
contains a collection of rib turbulators that are perpendicular and angled
with respect to the flow stream (Fig. 6) [26].

To determine the surface heat flux (used to calculate heat transfer coef-
ficients and Nusselt numbers), the convective power levels provided by the
thermofoil heaters are divided by flat test surface area. Spatially resolved
temperature distributions along the bottom rib turbulator test surface are
determined using liquid crystals thermography and true-colour image pro-
cessing system commercially available from Hallcrest [25].

The main part of PIV set-up as a part of wind tunnel consists of a trans-
parent model of ribbed channel, laser light source (30 mJ double pulse
Nd:YAG laser SoloPIV, New Wave Research, Inc.) and high resolution
12 bit digital CCD camera (1280×1024 pixels, PCO SensiCam). This sys-
tem permits acquisition of two images at the minimum time interval of
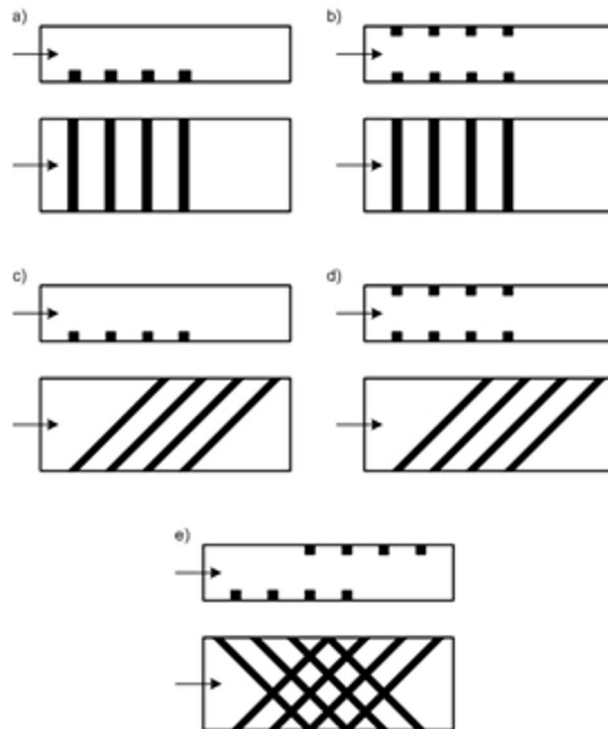200 ns, exposure time of 5 ns, and about 3.75 Hz repetition rate. The PIV

Figure 6: Schematic view of five types of transverse vortex generators (rectangular ribs).

recording system installed on 3 GHz Pentium 4 computer with 3 GB RAM capable for acquisition over 200 pairs of images during a single experimental run. The PIV measurements were performed for pure air seeded with small droplets (few micrometers in diameter) of synthetic oil DEHS (diethyl heksyl sebacat). The oil drops volumetric concentration was very low (< 0.001), hence they did not affect the flow structure.

For research of film cooling on a turbine blade the wind tunnel was modified, as well as new test section was constructed (Fig. 7). The geometry of test section in the form of a channel was made on the basis of numerical calculations. The tunnel was equipped with a bypass valve that allows the organization of air flow so that measurements can be taken in steady-state and transient states.

Figure 7: The view of test rig: wind tunnel and data acquisition system (left), test section and lighting system (right).

5   Selected results of thermographic and flow measurements

Below are presented selected results regarding TLC and PIV measurements for model geometries of channel with ribs shown in Fig. 6 as well as visualization by TLC of cooling of model turbine blades.

5.1   LCT and PIV measurements for model heat exchanger

Thermographic measurements of stationary temperature fields in the ribbed channel representing model heat exchanger were aimed at determining local heat transfer coefficients and the Nusselt number.

The surface temperature was evaluated on the basis of hue measurements (as an attribute of the HSI – hue, saturation, intensity colour models), which were then converted to Kelvin or Celsius temperature using the liquid crystal calibration curve. Using the measuring system, the reading of hue values and also temperature was carried out with the accuracy of one pixel along the measuring section.

Nusselt number distributions for channels with 10 mm width and transverse vortex generators (rib turbulators) for two of geometries in Fig. 6 for different Reynolds numbers (9 000; 16 000; 26 000; 35 500) in the boundary layer are shown in Figs. 8 and 9. The analysis of the boundary layer was carried out to assess the impact of the channel wall on heat transfer. Higher Nusselt numbers were obtained for configuration shown in Fig. 6b, as was
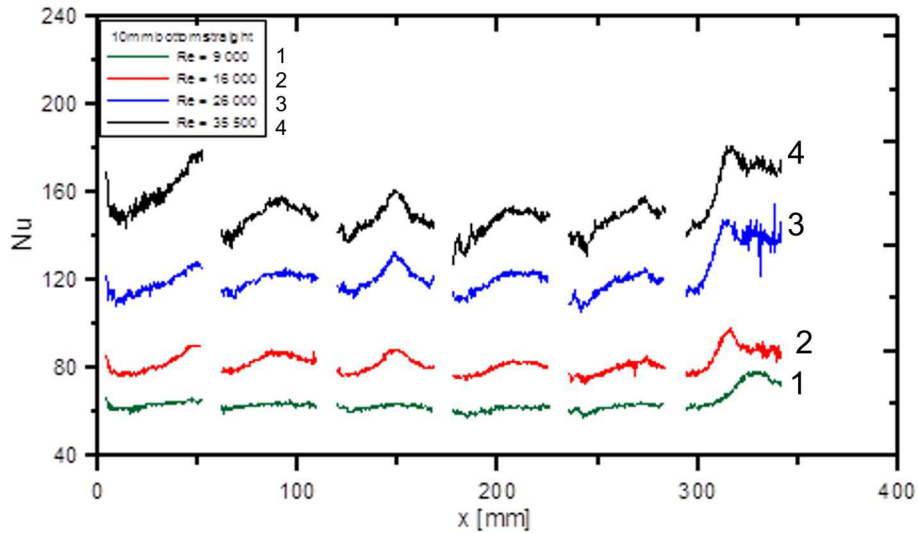
Figure 8: Local streamwise Nusselt number distribution in the middle part of the channel for different Reynolds numbers for configuration shown in Fig. 6a with ribbed bottom wall perpendicularly to the flow.
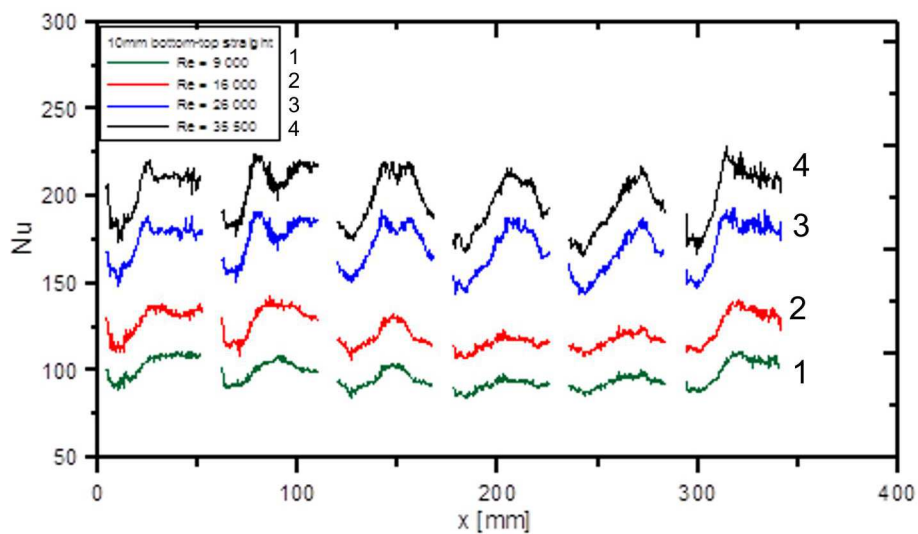

Figure 9: Local streamwise Nusselt number distribution in the middle part of the channel for different Reynolds numbers for Fig. 6b with ribbed bottom and top walls perpendicularly to the flow.

expected. More information can be found in [26].

Velocity fields in case of ribbed channel were obtained from the PIV measurements for different ribs configurations(Fig. 7) and different Reynolds numbers (Re = 9 000, 16 000, and 26 000). The area scanned by the PIV method was in all cases located in the mid-vertical-plane between side walls (one position of the laser light sheet).
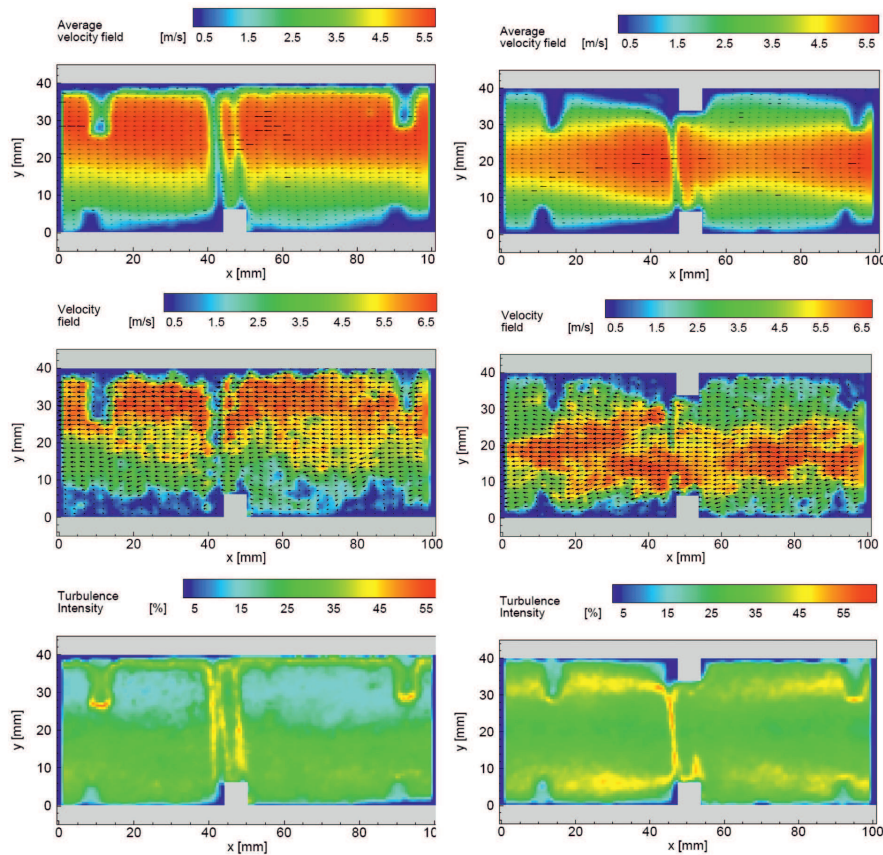

Figure 10: Average velocity field (up), instantaneous velocity field (middle) and turbulence intensity (bottom) for and Reynolds number 16 000 for configurations 6a (left) and 6b (right).

Figure 10 shows an average velocity field (averaged over 100 instantaneous velocity fields) for a configuration with ribbed bottom wall only (Fig. 6a) and with ribbed both walls (Fig. 6b) and flow perpendicular to the ribs. Ribs are 6 mm in width and height. Reynolds number is 16 000. Maximum

velocity for both cases is about 5.5 m/s and is located in the upper part of the channel for geometry 6a and in the middle part of the channel for geometry 6b. Turbulence intensity achieves about 55% for configuration 6a and about 60% for configuration 6b.

5.2   Visualization of film cooling of model turbine blades

Internal cooling technique for gas turbine blades has been studied for many years. The designers need detailed data for heat transfer and temperature distributions along with the flow and streamwise pressure gradient to understand the flow physics and to improve the current internal cooling designs. Examples of modified gas turbine blades are shown in Fig. 11 [27].

Figure 11: Gas turbine blades with cooling holes (left).

To visualize the process of model turbine blade cooling by air flow, liquid crystal thermography and computer analysis of colour images were used. Experimental research was carried out in the air tunnel, in which the measurement section was a model of inter-blade space of the turbine wheel. View of test section of low-speed wind tunnel is presented in Fig. 7. The position and shape of the model blade in the measuring space, the optimal diameters of the exhaust openings, angle of the column of the cooling air streams, the so-called jets in the direction of flow and the number and arrangement of jet outlets in relation to the incoming main air stream were

established according to actual turbine passage. Examples of steady-state and transient TLC measurements and visualization are shown in Figs. 12 and 13, respectively. Figure 12 presents temperature visualization along model blade for two different velocities of cooling jets, caused by different pressure between main and secondary (jets) air flow. The pressure ratio between cooling air and main stream was 5% for the left figure and 15% for the right one. Reynolds number for main flow was 122 000.
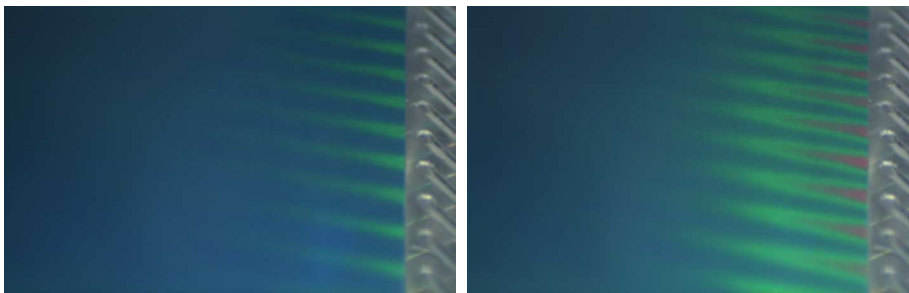

Figure 12: Steady-state TLC visualization of air flow on a blade surface with air jets for different secondary flow.

Figure 13 presents temperature visualization taken by TLC transient method. Measurements were performed for several time steps counted from the moment of influence of hot air to the measuring section. There is a 4 s time difference between left and right picture. Using history of temperature distribution heat transfer coefficient could be calculated.
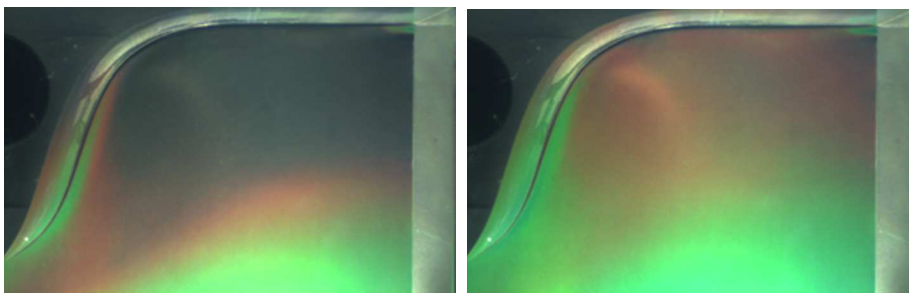

Figure 13: End-wall temperature distribution by transient TLC method for different time steps.

6 Conclusions

Novel transient and steady-state liquid crystal thermography technique were employed for two experimental research. First part of this work was dedicated to visualization of the hue value variations on the surface with square ribs and at the second part was devoted to maps of 2D temperature distribution along the model turbine blade with film cooling by air jets. Heat transfer distribution on the surface and the end-wall of a two-dimensional model cascade, caused by secondary flows, was evaluated. It stands now as a useful technique that allows new areas of research and new ways to thinking about heat transfer.

Computer aided analysis of colour images taken by particle image velocimetry also expand the range of possible experiments for fluid mechanics and complex geometries with highly non-uniform boundary conditions exposed to very aggressive flow fields.

Most of the studies and obtained data provide useful information for better understanding of thermal and flow performances of some selected technical applications.

References

[1] Mikielewicz D., Wajs J., Gliński M., Zrooga A.-B.R.S.: *Experimental investigation of dryout of SES 36, R134a, R123 and ethanol in vertical small diameter tubes.* Exp. Therm. Fluid Sci. **44**(2013), 556–564.

[2] Piasecka M., Strąk K., Maciejewska B.:: *Calculations of flow boiling heat transfer in a minichannel based on liquid crystal and infrared thermography data.* Heat Transfer Eng. **38**(2017), 3, 332–346.

[3] Wajs J., Mikielewicz D.: *Determination of dryout localization using a five-equation model of annular flow for boiling in minichannels.* Arch. Thermodyn. **38**(2017), 1, 123–139. DOI: 10.1515/aoter-2017-0007

[4] MIKIELEWICZ D., MIKIELEWICZ J., WAJS J., GLIŃSKI M.: *Modelling of dryout process in an annular flow*. Heat Transf. Res. **39**(2008), 7, 587–596. DOI: 10.1615/HeatTransRes.v39.i7.30

[5] REINITZER R.: *Beitrage zur Kenntniss des Cholestrins*. Monatschr. Chem. Wien **9**(1899), 421–441.

[6] MOFFAT R.J.: *Experimental heat transfer*. In: Proc. 9th Int. Heat Transfer Conf. Jerusalem **1**(1991), 308–310.

[7] JONES T.V., WANG Z., IRELAND P.T.: *The use of liquid crystals in aerodynamic and heat transfer experiments*. In: Proc. First I.Mech.E. Sem. on optical methods and Data Processing in Heat and Fluid Flow, City University London, 1992, 51–65.

[8] STASIEK J.: *Thermochromic liquid crystals and true-colour image processing in heat transfer and fluid flow research*. Heat and Mass Transfer **33**(1997), 27–39.

[9] STASIEK J.A., KOWALEWSKI T.A.: *Thermochromic liquid crystals applied for heat transfer research*. Optoelectronics Rev. **10**(2002), 1, 1–10.

[10] ZIEMBA A., FORNALIK-WAJS E.: *Evaluation of colour space transformation suitability to optical temperature measurements*. J. Physics Conf. Ser. **745**(2016), 032108. DOI:10.1088/1742-6596/745/3/032108

[11] STASIEK J., STASIEK A., JEWARTOWSKI M., COLLINS M.W.: *Liquid crystal thermography and true-colour digital image processing*. Opt. Laser Technol. **38**(2006), 243–256.

[12] AKINO N., KUNUGI T., ICHIMIYA K., MITSUCHIRO K., UEDA M.: *Improved liquid crystal thermography excluding human colour sensation*. ASME J.Heat Transfer **111**(1989), 558–565.

[13] STASIEK J., COLLINS M.W.: *The use of liquid crystals and true-colour image processing in heat and fluid flow experiments*. In: Atlas of Visualization II, CRC Press, 1996, 79–104.

[14] ABDULLAH N., ABU TALIB. A, JAAFAR, A.A., SALLEH, M.A.M., CHONG, W.T.: *The basics and issues of Thermochromic Liquid Crystal Calibrations*. Exp. Therm. Fluid Sci. **34**(2010), 1089–1121.

[15] SATTA F. SIMONI D., TANDA G.: *Experimental investigation of flow and heat transfer in a rectangular channel with 45° angled ribs on one/two walls*. Exp. Therm. Fluid Sci. **37**(2012), 46–56.

[16] LIU J., HUSSAIN S., WANG J., WANG L., XIE G., SUNDEN B.: *Heat transfer enhancement and turbulent flow in a high aspect ratio channel (4:1) with ribs of various truncation types and arrangements*. Int. J. Therm. Sci. **123**(2018), 99–116.

[17] SATTA F., TANDA G.: *Measurement of local heat transfer coefficient on the endwall of a turbine blade cascade by liquid crystal thermography*. Exp. Therm. Fluid Sci. **58**(2014), 209–215.

[18] FORNALIK E.: *Flow patterns generated by a strong magnetic field*. J. Theor. App. Mech-Pol **45**(2007), 3, 557–568.

[19] STASIEK J., JEWARTOWSKI M. AND KOWALEWSKI T.A.: *The use of liquid crystal thermography in selected technical and medical applications – recent development*. J. Crystal. Process Technol. **4**(2014), 46–59.

[20] FORNALIK E., SZMYD J.: *Experimental investigations of jet flows.* J. Theor. Appl. Mech-Pol **45**(2007), 3, 569–586.

[21] ABIDI-SAAD A., POLIDORI G., KADJA M., BEAUMONT F., POPA C.V., KORICHI A.: *Experimental investigation of natural convection in a vertical rib-roughened channel with asymmetric heating.* Mech. Res. Commun. **76**(2016), 1–10.

[22] LIOU T.M., CHANG S.W., CHAN S.P.: *Effect of rib orientation on thermal and fluid-flow features in a two-pass parallelogram channel with abrupt entrance.* Int. J. Heat. Mass Tran. **116**(2018), 152–165.

[23] ZHAI Y., XIA G., CHEN Z., LI Z.: *Micro-PIV study of flow and the formation of vortex in micro heat sinks with cavities and ribs.* Int. J. Heat Mass Tran. **98**(2016), 380–389.

[24] BLONSKI S., KORCZYK P.M., KOWALEWSKI T.A.: *Analysis of turbulence in a micro- channel emulsifier.* Int. J. Therm. Sci. **46**(2007), 11, 1126–1141.

[25] HALLCREST *Handbook of Thermochromic Liquid Crystal Technology* LCR Hallcrest, 2014.

[26] MIKIELEWICZ D., STASIEK A., JEWARTOWSKI M. AND STASIEK J.: *Measurements of heat transfer enhanced by the use of transverse vortex generators.* Appl. Therm. Eng. **49**(2012), 61–72.

[27] GIAMPAOLO A.: *Gas turbine handbook: principles and practices.* Fairmont Press, 2006.